



**HAL**  
open science

## Spectral minimal partitions of a sector

Virginie Bonnaillie-Noël, Corentin Léna

► **To cite this version:**

Virginie Bonnaillie-Noël, Corentin Léna. Spectral minimal partitions of a sector. *Discrete and Continuous Dynamical Systems - Series B*, 2014, 19 (1), pp.27-53. 10.3934/dcdsb.2014.19.27 . hal-00763467

**HAL Id: hal-00763467**

**<https://hal.science/hal-00763467v1>**

Submitted on 10 Dec 2012

**HAL** is a multi-disciplinary open access archive for the deposit and dissemination of scientific research documents, whether they are published or not. The documents may come from teaching and research institutions in France or abroad, or from public or private research centers.

L'archive ouverte pluridisciplinaire **HAL**, est destinée au dépôt et à la diffusion de documents scientifiques de niveau recherche, publiés ou non, émanant des établissements d'enseignement et de recherche français ou étrangers, des laboratoires publics ou privés.

# Spectral minimal partitions of a sector

V. Bonnaillie-Noël\*, and C. Léna†

December 10, 2012

## Abstract

In this article, we are interested in determining the spectral minimal  $k$ -partition for angular sectors. We first deal with the nodal cases for which we can determine explicitly the minimal partitions. Then, in the case where the minimal partitions are not given by eigenfunctions of the Dirichlet Laplacian, we analyze the possible topologies of the minimal partitions. We first exhibit symmetric minimal partitions by using mixed Dirichlet-Neumann Laplacian and then use a double covering approach to catch non symmetric candidates.

**Keywords.** Spectral theory, minimal partitions, nodal domains, Aharonov-Bohm Hamiltonian, numerical simulations, finite element method

**MSC classification.** 35B05, 35J05, 35P15, 49M25, 65F15, 65N25, 65N30.

## 1 Introduction

Let us first state the definition of a minimal partition and review briefly known results about this object. In the following,  $\Omega$  is an open, bounded, and connected set in  $\mathbb{R}^2$ . We assume that  $\partial\Omega$  satisfies some regularity properties. Following [15], we can for example assume that  $\partial\Omega$  is compact, piecewise  $C^{1,+}$  and that  $\Omega$  satisfies the uniform cone property.

**Definition 1.1** *For any integer  $k \geq 1$ , a  $k$ -partition is a finite set*

$$\mathcal{D} = \{D_i : 1 \leq i \leq k\}$$

*of open, connected and mutually disjoint subsets of  $\Omega$ . The  $D_i$ 's are called the domains of the  $k$ -partition. The  $k$ -partition  $\mathcal{D}$  is called strong if*

$$\text{Int} \left( \bigcup_{i=1}^k D_i \right) \setminus \partial\Omega = \Omega.$$

*The set of all  $k$ -partitions is denoted by  $\mathfrak{P}_k$ .*

*If we do not want to specify the number of domains, we simply speak of a partition.*

For any bounded open set  $\omega \in \mathbb{R}^2$ , the sequence  $(\lambda_k(\omega))_{k \geq 1}$  denotes the eigenvalues of the Dirichlet Laplacian on  $\omega$ , in increasing order and counted with multiplicity.

---

\*IRMAR, ENS Cachan Bretagne, Univ. Rennes 1, CNRS, UEB, av. Robert Schuman, F-35170 Bruz, France [virginie.bonnaillie@bretagne.ens-cachan.fr](mailto:virginie.bonnaillie@bretagne.ens-cachan.fr)

†Laboratoire de Mathématique d'Orsay, Université Paris-Sud, Bât. 425, F-91405 Orsay Cedex, France [corentin.lena@math.u-psud.fr](mailto:corentin.lena@math.u-psud.fr)

**Definition 1.2** With any  $k$ -partition  $\mathcal{D} = \{D_i : 1 \leq i \leq k\}$ , is associated the energy

$$\Lambda_k(\mathcal{D}) = \max_{1 \leq i \leq k} \lambda_1(D_i).$$

We are concerned in this paper with minimizing this energy for angular sectors.

**Definition 1.3** For any integer  $k \geq 1$ , we set

$$\mathfrak{L}_k(\Omega) = \inf_{\mathcal{D} \in \mathfrak{P}_k} \Lambda_k(\mathcal{D}).$$

A partition  $\mathcal{D} \in \mathfrak{P}_k$  such that  $\Lambda_k(\mathcal{D}) = \mathfrak{L}_k(\Omega)$  is called a minimal  $k$ -partition.

The following existence result was proved in [7, 9, 8].

**Theorem 1.4** For any integer  $k \geq 1$ , there exists a minimal  $k$ -partition of  $\Omega$ . Furthermore, minimal partitions are strong.

Similar existence results were previously proved in a more general setting in [6].

Let us now define a regular partition.

**Definition 1.5** If  $\mathcal{D} = \{D_i : 1 \leq i \leq k\}$  is a strong partition, its boundary set is defined by

$$N(\mathcal{D}) = \overline{\bigcup_{i=1}^k \Omega \cap \partial D_i}.$$

The partition  $\mathcal{D}$  is called regular if the following properties are satisfied:

- (i) The set  $N(\mathcal{D}) \cap \Omega$  is locally a  $\mathcal{C}^{1,1^-}$  curve, except in the neighborhood of a finite set  $\{X_i : 1 \leq i \leq n\}$ . The elements of this set are called interior singular points.
- (ii) For each  $1 \leq i \leq n$ , there is an integer  $\nu_i \geq 2$  such that in a neighborhood of  $X_i$ , the set  $N(\mathcal{D})$  is the union of  $\nu_i$  half curves of class  $\mathcal{C}^{1,+}$  meeting at  $X_i$ .
- (iii) The set  $N(\mathcal{D}) \cap \partial\Omega$  is finite. Its elements are called boundary singular points. If  $Z \in N(\mathcal{D}) \cap \partial\Omega$ , there is an integer  $\rho \geq 1$  such that in the neighborhood of  $Z$ , the set  $N(\mathcal{D})$  is the union of  $\rho$  half curves of class  $\mathcal{C}^{1,+}$  in  $\bar{\Omega}$  meeting  $\partial\Omega$  at  $Z$ .
- (iv) At each interior singular point, the half curves meet with equal angles.
- (v) At each boundary singular point, the half curves and  $\partial\Omega$  meet with equal angles.

As proved in [15], we have the following regularity result:

**Theorem 1.6** For any  $k \geq 1$ , minimal  $k$ -partitions are regular (up to zero capacity sets).

We give additional definitions that help us to describe the topology of a partition.

**Definition 1.7** Let  $\mathcal{D} = \{D_i : 1 \leq i \leq k\}$  be a strong partition. Two domains  $D_i$  and  $D_j$  are said to be neighbors if  $\text{Int}(\overline{D_i \cup D_j}) \setminus \partial\Omega$  is connected.

**Definition 1.8** A strong partition is called bipartite if one can color its domains, using only two colors, in such a way that two neighbors have a different color.

Let us recall some definitions and results from the spectral theory of the Laplacian. They are used throughout the paper. Let  $u$  be an eigenfunction for the Dirichlet Laplacian.

**Definition 1.9** We call nodal set of  $u$  the set

$$N(u) = \overline{\{x \in \Omega : u(x) = 0\}}.$$

The connected components of  $\Omega \setminus N(u)$  are called the nodal domains of  $u$ . The number of nodal domains is denoted by  $\mu(u)$ . The set

$$\{D_i : 1 \leq i \leq \mu(u)\},$$

where the  $D_i$ 's are the nodal domains of  $u$ , is a regular partition of  $\Omega$ , called the nodal partition associated with  $u$ .

The following result was proved by Courant (cf. [10]).

**Theorem 1.10** If  $k \geq 1$  and  $u$  is an eigenfunction associated with  $\lambda_k(\Omega)$ ,

$$\mu(u) \leq k.$$

Following [15], we introduce a new definition.

**Definition 1.11** Let  $k \geq 1$ . An eigenfunction  $u$  for the Dirichlet Laplacian associated with  $\lambda_k(\Omega)$  is said to be Courant-sharp if  $\mu(u) = k$ .

To give some upper-bound for  $\mathfrak{L}_k(\Omega)$ , it could be interesting to use  $k$ -partitions obtained from eigenfunctions. Thus, we introduce a new spectral element.

**Definition 1.12** For  $k \geq 1$ ,  $L_k(\Omega)$  is the smallest eigenvalue of the Dirichlet Laplacian that has an eigenfunction with  $k$  nodal domains. If there is no such eigenvalue, we set  $L_k(\Omega) = +\infty$ .

With this notation, Theorem 1.10 reads as the inequality

$$\lambda_k(\Omega) \leq L_k(\Omega).$$

We can now give two results of [15] that link minimal and nodal partitions.

**Theorem 1.13** A minimal partition  $\mathcal{D}$  is nodal if, and only if, it is bipartite.

**Theorem 1.14** For any integer  $k \geq 1$ ,

$$\lambda_k(\Omega) \leq \mathfrak{L}_k(\Omega) \leq L_k(\Omega).$$

Furthermore, if  $\mathfrak{L}_k(\Omega) = L_k(\Omega)$  or  $\lambda_k(\Omega) = \mathfrak{L}_k(\Omega)$ , then

$$\lambda_k(\Omega) = \mathfrak{L}_k(\Omega) = L_k(\Omega),$$

and in this case, any minimal  $k$ -partition is nodal.

Let us point out a few consequences of Theorem 1.14.

**Remark 1.15** A nodal partition associated with a Courant-sharp eigenfunction is minimal.

**Remark 1.16** *Minimal 2-partitions are nodal. Indeed, let  $u$  be an eigenfunction associated with  $\lambda_2(\Omega)$ . The function  $u$  is orthogonal to the eigenspace for  $\lambda_1(\Omega)$  and thus has at least two nodal domains. It has at most two nodal domains by Courant's theorem. It is therefore Courant-sharp, which implies that  $\mathfrak{L}_2(\Omega) = \lambda_2(\Omega)$  and that any minimal 2-partition of  $\Omega$  is nodal.*

In this article, we are concerned with the minimal  $k$ -partitions of angular sectors. For  $0 < \alpha \leq 2\pi$ , we set

$$\Sigma_\alpha = \{(\rho \cos \theta, \rho \sin \theta) : 0 < \rho < 1 \text{ and } -\frac{\alpha}{2} < \theta < \frac{\alpha}{2}\}.$$

This set is the circular sector of opening  $\alpha$ . We denote by  $(\lambda_k(\alpha))_{k \geq 1}$  the eigenvalues of the Dirichlet Laplacian on  $\Sigma_\alpha$ , in increasing order and counted with multiplicity. Due to the inclusion of the form domains and the min-max principle, the function  $\alpha \mapsto \lambda_k(\alpha)$  is decreasing for any  $k \geq 1$ .

In Section 2, we make explicit the spectrum of the Dirichlet Laplacian on  $\Sigma_\alpha$  and determine the minimal 2-partitions. In Section 3, we prove that for any  $k$ , the minimal  $k$ -partition is nodal as soon as  $\alpha$  is small enough. In Sections 4-6, we focus on the 3-partitions. First, we determine when the minimal 3-partition is nodal (Section 4). Then, Section 5 deals with non nodal symmetric minimal 3-partitions, with some remarks about the particular case  $\alpha = \pi/3$ . Then we use a double covering approach to exhibit some non symmetric candidates in Section 6. In this way, we find some non symmetric candidates which are better than any symmetric candidate. Finally we give in Section 7 some negative results for minimal  $k$ -partitions when  $k = 4, 5, 6$  and give configurations of partitions that are never minimal.

## 2 Nodal partitions

### 2.1 Explicit eigenmodes

**Proposition 2.1** *The eigenmodes  $(\lambda_{m,n}(\alpha), u_{m,n}^\alpha)$  of the Dirichlet Laplacian on the angular sector  $\Sigma_\alpha$  are given by*

$$\begin{aligned} \lambda_{m,n}(\alpha) &= j_{m\frac{\pi}{\alpha},n}^2, \\ u_{m,n}^\alpha(\rho, \theta) &= J_{m\frac{\pi}{\alpha}}(j_{m\frac{\pi}{\alpha},n}\rho) \sin(m\pi(\frac{\theta}{\alpha} + \frac{1}{2})), \end{aligned}$$

where  $j_{m\frac{\pi}{\alpha},n}$  is the  $n$ -th positive zero of the Bessel function of the first kind  $J_{m\frac{\pi}{\alpha}}$ .

**Proof:** These rather classical results are presented for example in [10]. One can compute the eigenvalues of the Dirichlet Laplacian on  $\Sigma_\alpha$  by separation of variables. In polar coordinates, the Laplacian reads

$$-\partial_\rho^2 - \frac{1}{\rho} \partial_\rho - \frac{1}{\rho^2} \partial_\theta^2.$$

We look for a solution  $(\lambda, u)$  of

$$\begin{cases} -\Delta u &= \lambda u & \text{in } \Sigma_\alpha, \\ u &= 0 & \text{on } \partial\Sigma_\alpha, \end{cases}$$

where  $\lambda > 0$  and  $u$  is not identically zero. If we set  $u(\rho, \theta) = \varphi(\rho)\psi(\theta)$ , this yields

$$-\frac{\psi''(\theta)}{\psi(\theta)} = \frac{\rho^2}{\varphi(\rho)} \left( \varphi''(\rho) + \frac{1}{\rho} \varphi'(\rho) + \lambda \varphi(\rho) \right).$$

According to the Dirichlet conditions,  $\psi(-\frac{\alpha}{2}) = \psi(\frac{\alpha}{2}) = 0$ . Therefore there exists an integer  $m \geq 1$  such that, up to a constant multiplicative factor,

$$\psi(\theta) = \sin\left(\frac{m\pi}{\alpha}\left(\theta + \frac{\alpha}{2}\right)\right).$$

Then, we get

$$\varphi''(\rho) + \frac{1}{\rho}\varphi'(\rho) + \left(\lambda - \frac{m^2\pi^2}{\alpha^2\rho^2}\right)\varphi(\rho) = 0.$$

If we set

$$\nu = \frac{\pi}{\alpha}, \quad \lambda = \omega^2, \quad t = \omega\rho, \quad f(t) = \varphi(\rho),$$

we recognize the Bessel differential equation

$$f''(t) + \frac{1}{t}f'(t) + \left(1 - \frac{m^2\nu^2}{t^2}\right)f(t) = 0.$$

The function  $u$  is assumed to be in  $H^1(\Sigma_\alpha)$  and to satisfy the Dirichlet boundary condition. This implies that  $f$  is proportional to the Bessel function of the first kind  $J_{m\nu}$  and that  $\omega$  is a zero of  $J_{m\nu}$ .

We have obtained a family of eigenmodes  $(\lambda_{m,n}(\alpha), u_{m,n}^\alpha)$  indexed by  $m \geq 1$  and  $n \geq 1$ . More precisely, we have the expressions

$$\lambda_{m,n}(\alpha) = j_{m\nu,n}^2, \tag{2.1}$$

where  $j_{m\nu,n}$  is the  $n$ -th positive zero of the function  $J_{m\nu}$  and

$$u_{m,n}^\alpha(\rho, \theta) = J_{m\nu}(j_{m\nu,n}\rho) \sin(m\nu(\theta + \frac{\alpha}{2})). \tag{2.2}$$

We can check that the set  $\{u_{m,n}^\alpha\}_{m,n}$  is orthogonal and spans  $L^2(\Sigma_\alpha)$ . Therefore there is no other eigenvalue.  $\blacksquare$

**Corollary 2.2** *For any  $k \geq 2$  and  $\alpha \in (0, 2\pi]$ , we have the first estimate*

$$\lambda_k(\alpha) \leq \mathfrak{L}_k(\alpha) \leq L_k(\Sigma_\alpha) \leq \inf\{\lambda_{m,n}(\alpha) : mn = k\}.$$

**Proof:** It is enough to use Theorem 1.14, Proposition 2.1 and to notice that for any  $m \geq 1, n \geq 1$ , and  $\alpha \in (0, 2\pi]$ , the eigenfunction  $u_{m,n}^\alpha$  has  $mn$  nodal domains.  $\blacksquare$

In Figure 1 are plotted some eigenvalues  $\lambda_{m,n}(\alpha)$  for  $1 \leq m \leq 7, 1 \leq n \leq 4$ , and  $\alpha \in (0, 2\pi]$ .

## 2.2 Minimal nodal partition

**Proposition 2.3** *For  $2 \leq k \leq 5$ , we define*

$$\alpha_k^2 = \inf\{\alpha \in (0, 2\pi] : \lambda_{k,1}(\alpha) < \lambda_{1,2}(\alpha)\}.$$

*Then for any  $\alpha \in [\alpha_k^2, 2\pi]$ , the nodal partition associated with  $u_{k,1}^\alpha$  is a minimal  $k$ -partition and we have*

$$\mathfrak{L}_k(\Sigma_\alpha) = \lambda_{k,1}(\alpha).$$

*For  $2 \leq k \leq 5$  and  $\alpha \in (\alpha_k^2, 2\pi]$ , the minimal  $k$ -partition consists then of  $k$  angular sectors with the same aperture.*

*For  $k \geq 6$ , any  $k$ -partition constituted of  $k$  angular sectors is never minimal.*

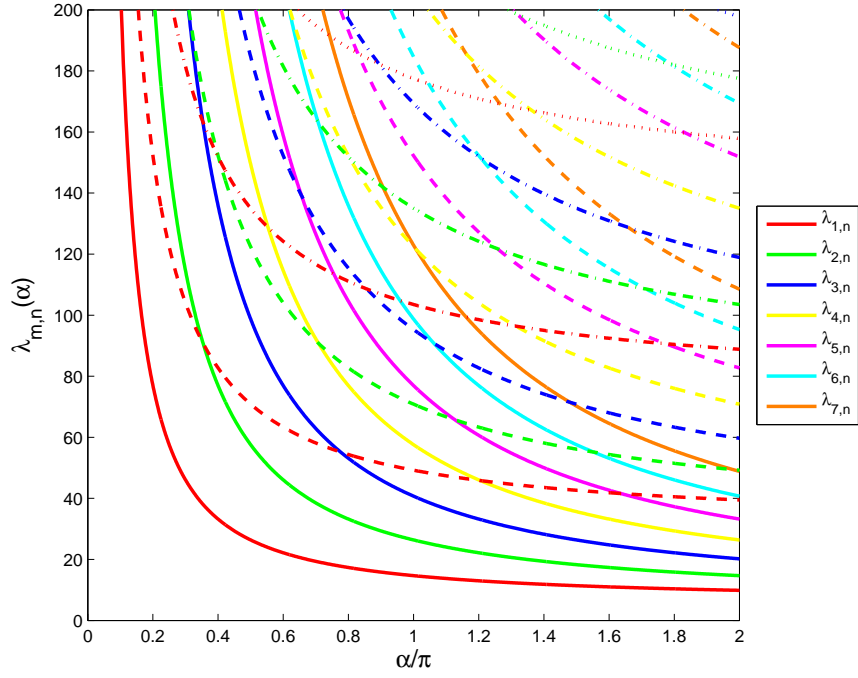


Figure 1:  $\lambda_{m,n}(\alpha)$  vs.  $\alpha/\pi$  for  $1 \leq m \leq 7$ ,  $1 \leq n \leq 4$ .

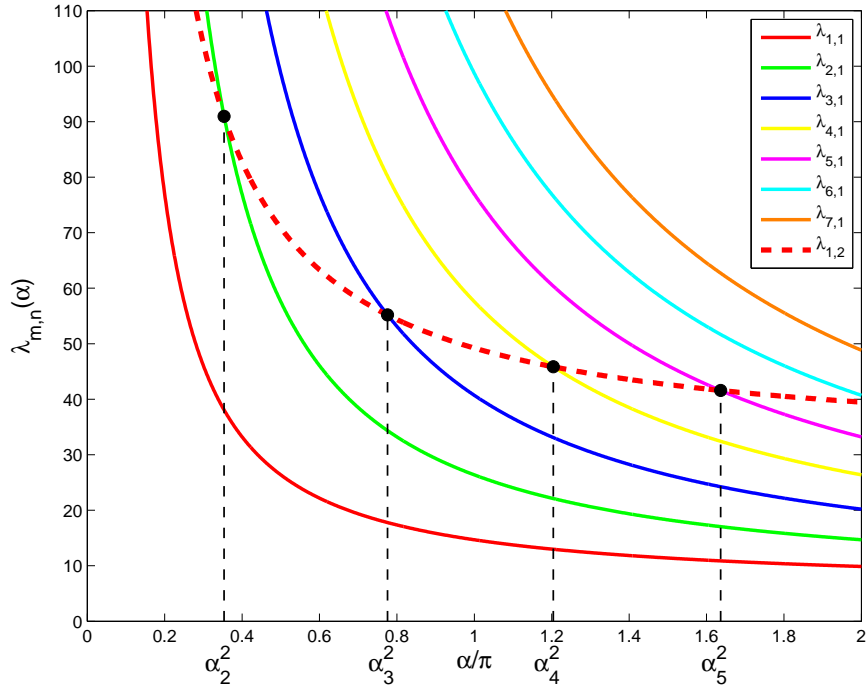


Figure 2:  $\lambda_{m,1}(\alpha)$  vs.  $\alpha/\pi$  for  $1 \leq m \leq 7$ , compared with  $\lambda_{1,2}(\alpha)$ .

**Proof:** Let us use (2.1) and look at Figure 2 where  $\lambda_{m,1}(\alpha)$  is compared with  $\lambda_{1,2}(\alpha)$ . We have

$$\lambda_{k,1}(2\pi) < \lambda_{1,2}(2\pi) \quad \text{for } k = 2, \dots, 5.$$

By continuity of  $\alpha \mapsto \lambda_{k,1}(\alpha)$ , the real number  $\alpha_k^2$  is well defined for  $2 \leq k \leq 5$ , and for any  $\alpha \in (\alpha_k^2, 2\pi]$ , we have

$$\lambda_{k,1}(\alpha) < \lambda_{1,2}(\alpha) \quad \text{for } k = 2, \dots, 5.$$

Using the definition of  $\alpha_k^2$ , we have

$$\lambda_k(\alpha) = \lambda_{k,1}(\alpha), \quad \forall \alpha \in (\alpha_k^2, 2\pi].$$

Since  $u_{k,1}^\alpha$  has  $k$  nodal domains, it is Courant-sharp and its nodal partition, composed of  $k$  equal angular sectors, is minimal according to Remark 1.15.

For  $k \geq 6$ , we observe that  $\lambda_{k,1}(\alpha) > \lambda_{1,2}(\alpha)$  for any  $\alpha \in (0, 2\pi]$ . Then  $\lambda_{k,1}(\alpha) > \lambda_k(\alpha)$ , the eigenfunction  $u_{k,1}^\alpha$  is not Courant-sharp, and its nodal partition is not minimal.

Still assuming  $k \geq 6$ , let us prove by contradiction that a  $k$ -partition  $\mathcal{D}_k = (D_1, \dots, D_k)$  with  $D_i$  angular sector cannot be minimal. Let us assume that it is minimal. Then the aperture for each sector must be the same, otherwise we could decrease the energy by increasing some angles and decreasing others. The partition  $\mathcal{D}_k$  is therefore nodal, associated with  $u_{k,1}$ , and thus not minimal.  $\blacksquare$

### 2.3 Minimal 2-partition

According to Remark 1.16, we know that

$$\mathfrak{L}_2(\Sigma_\alpha) = \lambda_2(\alpha), \quad \forall 0 < \alpha \leq 2\pi.$$

Furthermore a minimal 2-partition is given by the nodal partition associated with  $\lambda_2(\alpha)$ . To be more precise, for  $\alpha < \alpha_2^2$ ,  $\lambda_2(\alpha)$  is simple and equal to  $\lambda_{1,2}(\alpha)$  and for  $\alpha > \alpha_2^2$ ,  $\lambda_2(\alpha)$  is simple and equal to  $\lambda_{2,1}(\alpha)$ . For  $\alpha < \alpha_2^2$  and  $\alpha > \alpha_2^2$ , there is a unique minimal 2-partition, given by the nodal domains of  $u_{1,2}^\alpha$  and  $u_{2,1}^\alpha$  respectively. Thus we have

#### Proposition 2.4

$$\mathfrak{L}_2(\Sigma_\alpha) = \begin{cases} \lambda_{1,2}(\alpha) & \text{for } 0 < \alpha \leq \alpha_2^2, \\ \lambda_{2,1}(\alpha) & \text{for } \alpha_2^2 \leq \alpha \leq 2\pi. \end{cases}$$

Figure 3 gives the unique minimal 2-partition when  $\alpha \neq \alpha_2^2$ .

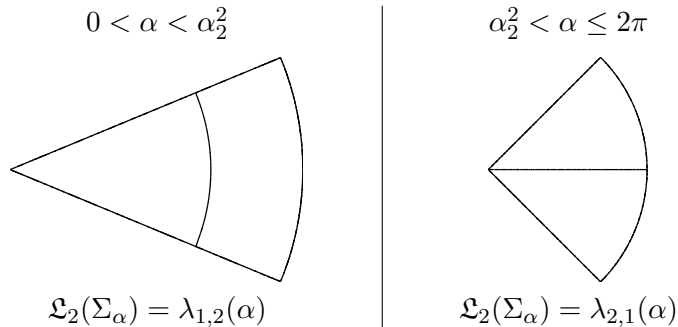


Figure 3: Minimal 2-partition on  $\Sigma_\alpha$ .

We notice that the eigenfunction  $u_{1,2}^\alpha$  is symmetric according to the axis  $\{y = 0\}$  while  $u_{2,1}^\alpha$  is antisymmetric.



Let us determine  $\alpha_2^2$  and the associated eigenvalue. We set  $\nu = \pi/\alpha_2^2$  and  $j = j_{\nu,2} = j_{2\nu,1}$ . The pair  $(\nu, j)$  is a solution of the (nonlinear) system

$$\begin{cases} J_\nu(j) &= 0, \\ J_{2\nu}(j) &= 0. \end{cases}$$

We can solve this system numerically by any iterative method. The initial values must be chosen so that  $j$  is indeed the second zero of  $J_\nu$  and the first of  $J_{2\nu}$ . In practice we find approximations of  $j$  and  $\nu$  thanks to Figure 2 and use them as initial values. We get

$$\begin{aligned} \alpha_2^2 &\simeq 0.3541 \pi \simeq 1.1125, \\ \lambda_2(\alpha_2^2) &\simeq 90.7745. \end{aligned}$$

For  $\alpha = \alpha_2^2$ ,  $\lambda_2(\alpha) = \lambda_{1,2}(\alpha) = \lambda_{2,1}(\alpha)$  has a two-dimensional eigenspace and the nodal domains of any nonzero linear combination of  $u_{1,2}^\alpha$  and  $u_{2,1}^\alpha$  give a minimal 2-partition (see Figure 4).

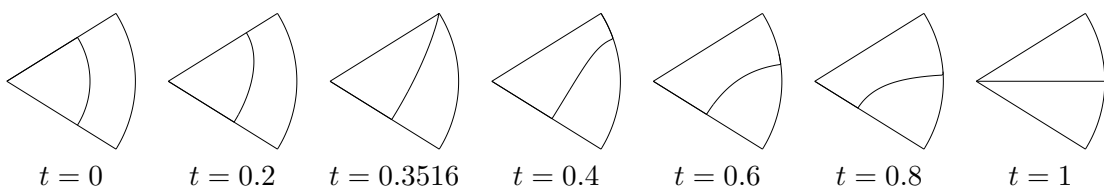


Figure 4: Minimal 2-partitions obtained as nodal partitions of  $(1-t)u_{1,2}^\alpha + tu_{2,1}^\alpha$ ,  $\alpha = \alpha_2^2$ .

### 3 Minimal partition for small angles

For sufficiently small angles, the minimal  $k$ -partition is nodal as explained in the following proposition.

**Proposition 3.1** *Let  $k \geq 2$ , we define*

$$\alpha_k^1 := \inf\{\alpha \in (0, 2\pi] : \lambda_{1,k}(\alpha) \geq \lambda_{2,1}(\alpha)\}. \quad (3.1)$$

*Then  $\alpha_k^1 > 0$  and for any  $0 < \alpha < \alpha_k^1$ , there is a unique minimal  $k$ -partition of  $\Sigma_\alpha$ , which is nodal, and more precisely consists of the nodal sets of  $u_{1,k}^\alpha$ .*

**Proof:** Using [11], we determine the asymptotic expansion of the  $n$ -th zero  $j_{\tilde{\nu},n}$  of the Bessel function  $J_{\tilde{\nu}}$  for large  $\tilde{\nu}$  :

$$j_{\tilde{\nu},n} = \tilde{\nu} - 2^{-1/3} a_n \tilde{\nu}^{1/3} + \mathcal{O}(\tilde{\nu}^{-1/3}).$$

Here  $a_n$  is the  $n$ -th negative zero of the Airy function  $Ai$ . Together with equation (2.1) and the relation  $\tilde{\nu} = m\pi/\alpha$ , this yields an asymptotic expansion for the eigenvalues :

$$\lambda_{m,n}(\alpha) = \frac{m^2 \pi^2}{\alpha^2} + 2^{2/3} |a_n| \left(\frac{m\pi}{\alpha}\right)^{4/3} + \mathcal{O}(\alpha^{-2/3}). \quad (3.2)$$

Let  $k \geq 2$  be an integer. The asymptotic expansion (3.2) implies that for  $\alpha$  small enough,  $\lambda_{1,k}(\alpha) < \lambda_{2,1}(\alpha)$ . Then the real number  $\alpha_k^1$  defined by relation (3.1) is strictly positive. For  $\alpha \in (0, \alpha_k^1)$ , we have  $\lambda_{1,k}(\alpha) < \lambda_{2,1}(\alpha)$  and therefore the first  $k$  eigenvalues of

the Dirichlet Laplacian on  $\Sigma_\alpha$  are  $\lambda_{1,1}(\alpha), \dots, \lambda_{1,k}(\alpha)$ . These eigenvalues are simple. Let  $u_{1,1}^\alpha, \dots, u_{1,k}^\alpha$  be the associated eigenfunctions defined by (2.2). The eigenfunction  $u_{1,k}^\alpha$  has  $k$  nodal domains and therefore is Courant-sharp. According to Theorem 1.15, the nodal partition associated with  $u_{1,k}^\alpha$  is minimal. Furthermore, the eigenspace associated with  $\lambda_{1,k}^\alpha$  has dimension 1 and thus this partition is unique. ■

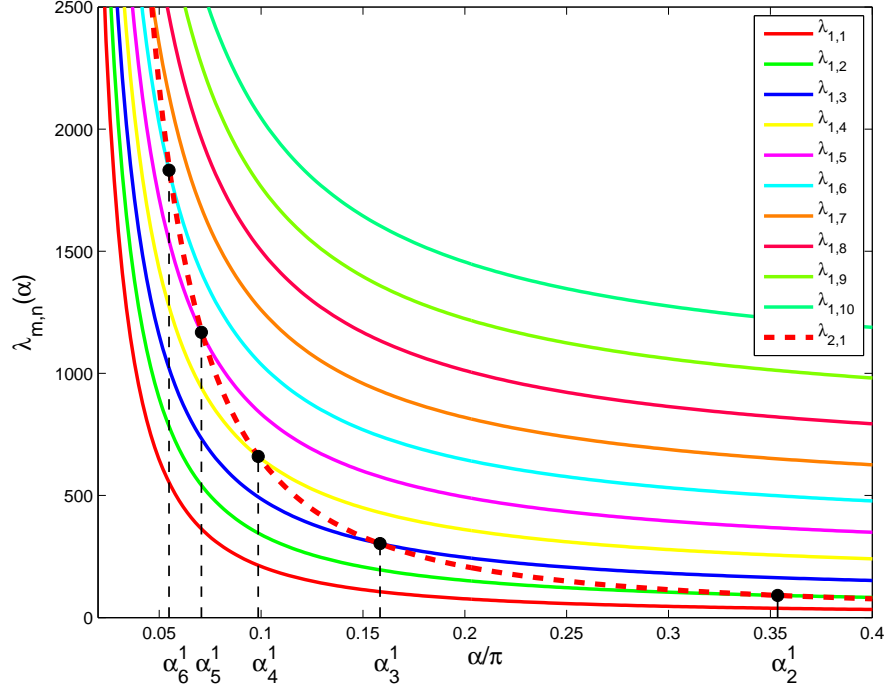


Figure 5:  $\lambda_{1,k}(\alpha)$  vs.  $\alpha/\pi$  for  $1 \leq k \leq 10$ , compared with  $\lambda_{2,1}(\alpha)$ .

Figure 5 gives the first ten eigenvalues  $\lambda_{1,k}(\alpha)$  compared with  $\lambda_{2,1}(\alpha)$  and shows the critical angles  $\alpha_k^1$ . We have

$$\begin{aligned} \alpha_2^1 &= \alpha_2^2, \\ \alpha_k^1 &< \alpha_k^2, \quad \text{for } k = 3, \dots, 5. \end{aligned}$$

We deduce

**Proposition 3.2** *For any  $2 \leq k \leq 5$ ,*

$$\begin{aligned} \mathfrak{L}_k(\Sigma_\alpha) &= \lambda_k(\alpha), \quad \forall \alpha \in (0, \alpha_k^1] \cup [\alpha_k^2, 2\pi], \\ \lambda_k(\alpha) &< \mathfrak{L}_k(\Sigma_\alpha) < L_k(\alpha), \quad \forall \alpha \in (\alpha_k^1, \alpha_k^2). \end{aligned}$$

**Remark 3.3** *Using the asymptotic expansion, we deduce that  $\lambda_{1,k}(\alpha) \leq \lambda_{k,1}(\alpha)$  as soon as  $\alpha$  is small enough. Let  $k$  be a prime number, we define*

$$\beta_k = \inf\{\alpha \in (0, 2\pi] : \lambda_{1,k}(\alpha) \geq \lambda_{k,1}(\alpha)\}. \quad (3.3)$$

Then, we have  $\beta_2 = \alpha_2^1 = \alpha_2^2$  and

$$L_k(\Sigma_\alpha) \leq \begin{cases} \lambda_{1,k}(\alpha) & \text{if } 0 < \alpha \leq \beta_k, \\ \lambda_{k,1}(\alpha) & \text{if } \beta_k \leq \alpha \leq 2\pi. \end{cases}$$

## 4 Minimal nodal 3-partition

As in the case of the 2-partition, we estimate numerically the transition angles  $\alpha_3^1$ ,  $\alpha_3^2$ ,  $\beta_3$ :

$$\begin{aligned} \alpha_3^1 &\simeq 0.1579 \pi \simeq 0.4961, & \lambda_3(\alpha_3^1) &\simeq 303.9139, \\ \alpha_3^2 &\simeq 0.7761 \pi \simeq 2.4382, & \lambda_3(\alpha_3^2) &\simeq 55.1671, \\ \beta_3 &\simeq 0.3533 \pi \simeq 1.1098, & L_3(\beta_3) &\simeq 163.3786. \end{aligned}$$

Proposition 3.2 and Remark 3.3 give estimates for  $\mathfrak{L}_3(\Sigma_\alpha)$  illustrated in Figure 6:

- for  $0 < \alpha \leq \alpha_3^1$ ,  $\mathfrak{L}_3(\Sigma_\alpha) = \lambda_3(\alpha) = \lambda_{1,3}(\alpha)$ ,
- for  $\alpha_3^1 < \alpha \leq \beta_3$ ,  $\lambda_{2,1}(\alpha) = \lambda_3(\alpha) < \mathfrak{L}_3(\Sigma_\alpha) < L_3(\Sigma_\alpha) = \lambda_{1,3}(\alpha)$ ,
- for  $\beta_3 \leq \alpha \leq \beta_2$ ,  $\lambda_{2,1}(\alpha) = \lambda_3(\alpha) < \mathfrak{L}_3(\Sigma_\alpha) < L_3(\Sigma_\alpha) = \lambda_{3,1}(\alpha)$ ,
- for  $\beta_2 \leq \alpha < \alpha_3^2$ ,  $\lambda_{1,2}(\alpha) = \lambda_3(\alpha) < \mathfrak{L}_3(\Sigma_\alpha) < L_3(\Sigma_\alpha) = \lambda_{3,1}(\alpha)$ ,
- for  $\alpha_3^2 \leq \alpha \leq 2\pi$ ,  $\mathfrak{L}_3(\Sigma_\alpha) = \lambda_3(\alpha) = \lambda_{3,1}(\alpha)$ .

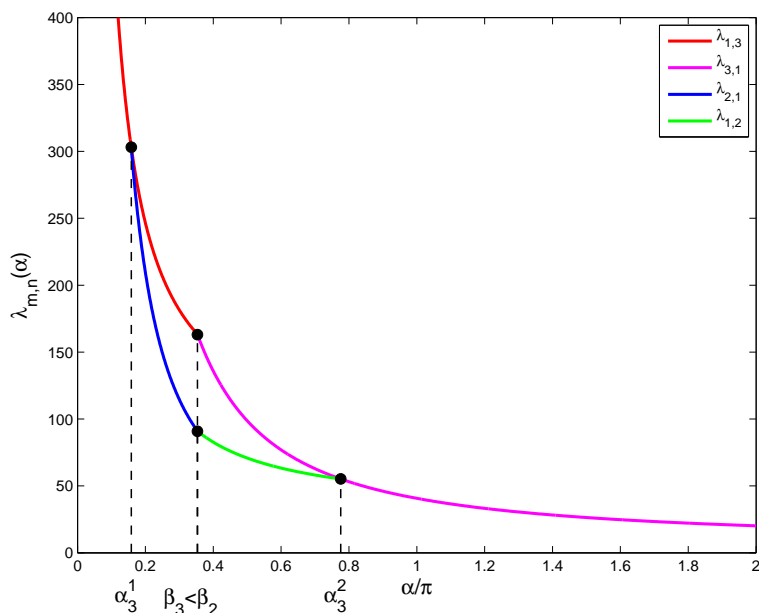


Figure 6: Lower and upper bounds for  $\mathfrak{L}_3(\Sigma_\alpha)$ .

If  $\alpha \leq \alpha_3^1$  or  $\alpha \geq \alpha_3^2$ , the eigenvalue  $\lambda_3(\alpha)$  has a Courant-sharp eigenfunction. According to Remark 1.15,  $\mathfrak{L}_3(\Sigma_\alpha) = \lambda_3(\alpha)$  and the minimal 3-partition is nodal, given by the nodal sets of an eigenfunction associated with  $\lambda_3(\alpha)$ . On the other hand, if  $\alpha_3^1 < \alpha < \alpha_3^2$ , no minimal 3-partition is nodal. Table 1 gives the nodal partition associated with the third eigenfunction. We notice that the eigenfunctions  $u_{1,3}^\alpha$  and  $u_{3,1}^\alpha$  are symmetric according to the axis  $\{y = 0\}$ .

Let us now look at the transition angles  $\alpha_3^1$  and  $\alpha_3^2$ . For such angles, the minimal 3-partition is no more unique.

Figure 7 represents the nodal partitions of some linear combination  $(1-t)u_{1,3}^\alpha + tu_{2,1}^\alpha$  for  $\alpha = \alpha_3^1$ . We observe a transition between a 2-partition and a 3-partition. When we have

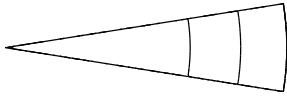
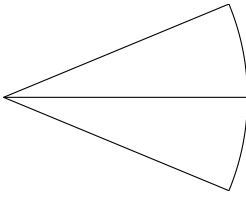
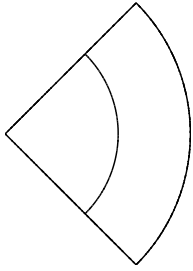
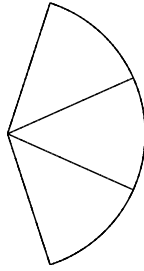
$0 < \alpha \leq \alpha_3^1$	$\alpha_3^1 < \alpha < \alpha_2^1$	$\alpha_2^1 < \alpha < \alpha_3^2$	$\alpha_3^1 \leq \alpha \leq 2\pi$
			
$\mathfrak{L}_3(\Sigma_\alpha) = \lambda_{1,3}(\alpha)$ <i>minimal 3-partition</i>	$\lambda_{2,1}(\alpha) < \mathfrak{L}_3(\Sigma_\alpha)$	$\lambda_{1,2}(\alpha) < \mathfrak{L}_3(\Sigma_\alpha)$	$\mathfrak{L}_3(\Sigma_\alpha) = \lambda_{3,1}(\alpha)$ <i>minimal 3-partition</i>

Table 1: Nodal partition associated with  $\lambda_3(\alpha)$  on  $\Sigma_\alpha$ .

a 3-partition, it is a minimal one since the eigenfunction is associated with  $\lambda_3(\alpha)$  and then Courant-sharp (see Remark 1.15). Notice that the function  $u_{1,3}^\alpha$  is symmetric with respect to the  $y$ -axis whereas the function  $u_{2,1}^\alpha$  is antisymmetric. Thus, by considering linear combinations, we break the symmetry of the 3-partition and exhibit some minimal 3-partitions which are non symmetric.

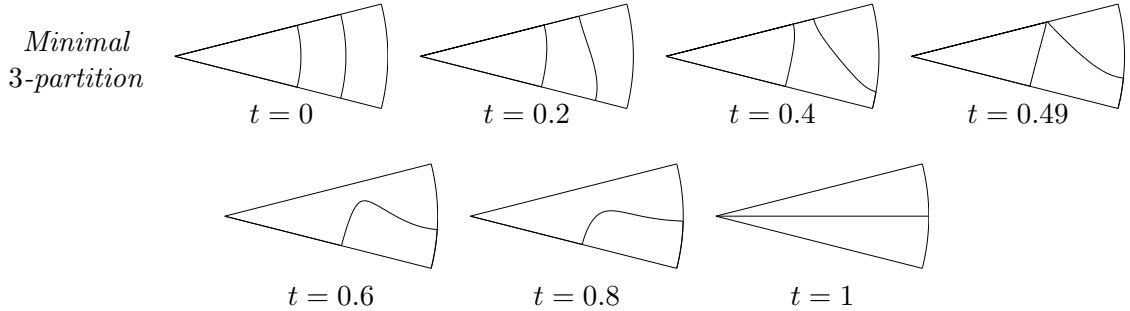


Figure 7: Nodal partitions of  $(1-t)u_{1,3}^\alpha + tu_{2,1}^\alpha$ ,  $\alpha = \alpha_3^1$ .

The following proposition gives information about the transition in the linear combinations between 2-partition and 3-partition.

**Proposition 4.1** *There are eigenfunctions associated with  $\lambda_3(\alpha_3^1)$  whose nodal set has a boundary singular point with two nodal lines which hit at this point. The polar coordinates of this boundary singular point is either  $(\rho_c, \alpha_3^1/2)$  or  $(\rho_c, -\alpha_3^1/2)$  with  $\rho_c \simeq 0.6558$ .*

**Proof:** We recall that

$$\lambda_3(\alpha_3^1) = \lambda_{1,3}(\alpha_3^1) = \lambda_{2,1}(\alpha_3^1).$$

We set

$$\nu = \frac{\pi}{\alpha_3^1}, \quad j = j_{\nu,3} = j_{2\nu,1}.$$

Any associated eigenfunction is of the form

$$u(\rho, \theta) = aJ_\nu(j\rho) \cos(\nu\theta) + bJ_{2\nu}(j\rho) \sin(2\nu\theta),$$

where  $a$  and  $b$  are coefficients to be determined. It can be factorized as

$$u(\rho, \theta) = J_{2\nu}(j\rho) \cos(\nu\theta) \left( a \frac{J_\nu(j\rho)}{J_{2\nu}(j\rho)} + 2b \sin(\nu\theta) \right).$$

Let us define

$$v(\rho, \theta) = a \frac{J_\nu(j\rho)}{J_{2\nu}(j\rho)} + 2b \sin(\nu\theta).$$

We are looking for values of  $a$  and  $b$  for which  $v$  has a zero that is also a singular point. The equation  $\nabla v(\rho, \theta) = 0$  can be solved and yields

$$\begin{cases} \theta_c &= \pm\alpha_3^1/2, \\ \rho_c &\simeq 0.6558. \end{cases}$$

Thanks to the equation  $v(\theta_c, \rho_c) = 0$ , we then find  $a$  and  $b$  up to a common multiplicative factor. ■

Similarly, Figure 8 gives the nodal partition associated with the linear combination  $(1-t)u_{1,2}^\alpha + tu_{3,1}^\alpha$  for  $\alpha = \alpha_3^2$ . In this case, the functions  $u_{1,2}$  and  $u_{3,1}$  are both symmetric with respect to the  $y$ -axis. Then any linear combination satisfies this symmetry too. As previously, we observe a transition between a 2-partition and a 3-partition. When we have a 3-partition, it is still a minimal one. We can characterize the transition between 2-partition and 3-partition:

**Proposition 4.2** *There are eigenfunctions associated with  $\lambda_3(\alpha_3^2)$  for which the point of coordinates  $(1,0)$  is a boundary singular point. Two nodal lines meet at this point.*

**Proof:** This proposition is proved in the same way than proposition 4.1. ■

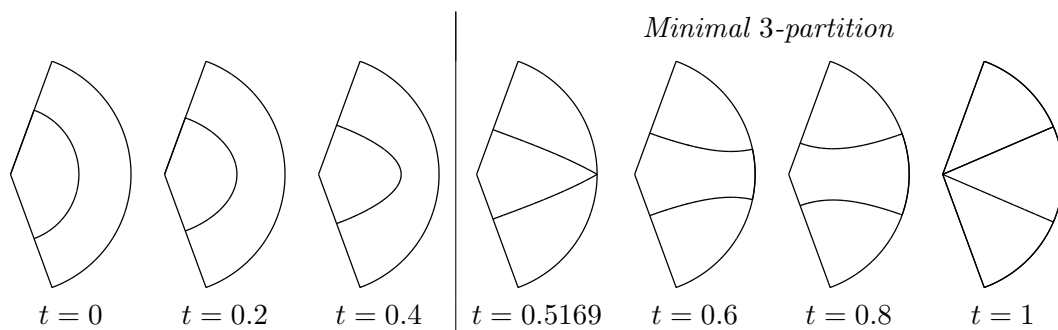


Figure 8: Nodal partition of  $(1-t)u_{1,2}^\alpha + tu_{3,1}^\alpha$ ,  $\alpha = \alpha_3^2$ .

## 5 Minimal symmetric 3-partitions

In this section, we propose candidates to be minimal symmetric 3-partitions. This approach was used in [5] to catch symmetric candidates for the square and the disk.

Looking at nodal minimal 3-partitions obtained in Section 4, we observe that for any  $\alpha \in (0, \alpha_3^1] \cup [\alpha_3^2, 2\pi]$ , there exists a symmetric minimal 3-partition. Now, we exhibit symmetric candidates to be minimal symmetric 3-partitions for  $\alpha \in (\alpha_3^1, \alpha_3^2)$ . We refer to [5] to explain the possible symmetric configurations. Using the Euler formula (cf. [14]), there are only three configurations, represented in Figure 9, for the minimal 3-partition when  $\alpha_3^1 < \alpha < \alpha_3^2$ :

- (a) The 3-partition has one interior singular point  $X_0$ , which is necessarily on the symmetry axis.
- (b) The 3-partition has two interior singular points  $X_0, X_1$  and no boundary singular point.
- (c) The 3-partition has two interior singular points and two boundary singular points. Moreover  $\partial D_1 \cap \partial D_2$  consists of two curves, each one joining one boundary singular point to one interior singular point.

In configurations (b) and (c), the interior singular points  $X_0, X_1$  (and boundary singular points for case (c)) are either on the symmetry axis, or symmetric to each other.

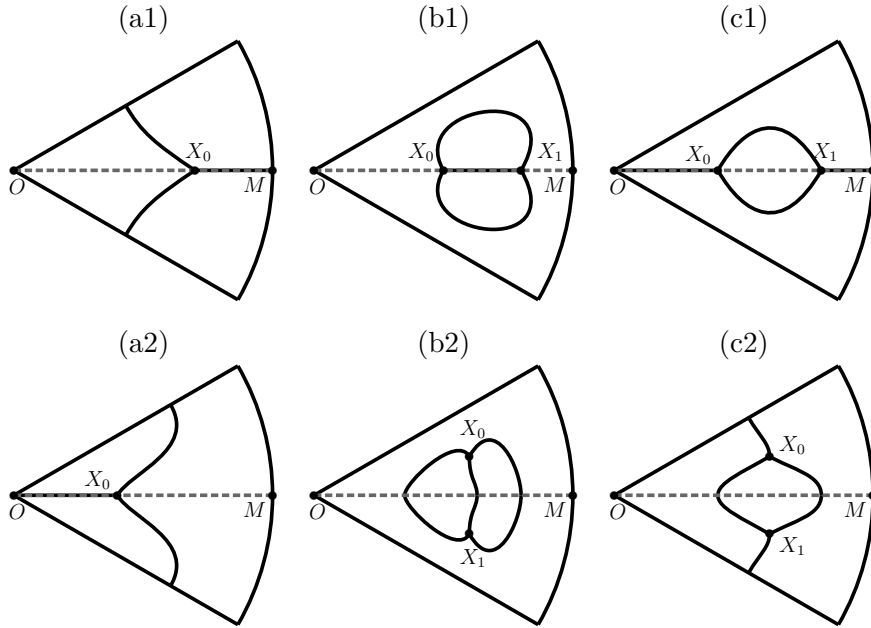


Figure 9: Configuration of the non bipartite symmetric minimal 3-partition.

### 5.1 Partition with one interior singular point

Let us first consider configurations of type (a). To catch such configuration, it is enough to deal with the half-domain  $\Sigma_\alpha^+ = \Sigma_\alpha \cap \{y > 0\}$  and look at 2-partitions on this half-domain. The main advantage is that the minimal 2-partitions are nodal; to determine them, it is enough to compute the second eigenfunction. The unknown parameter is the position of the singular point  $X_0^\alpha$ . Thus we compute the second eigenvector of the Neumann-Dirichlet and Dirichlet-Neumann Laplacian on  $\Sigma_\alpha^+$  and move the singular point all along the axis  $\{y = 0\}$ ; we denote by  $x_\alpha$  the abscissa of the singular point  $X_0^\alpha$  and by  $\lambda_2^{ND}(x_\alpha)$  and  $\lambda_2^{DN}(x_\alpha)$  the second eigenvalue of the Neumann-Dirichlet and Dirichlet-Neumann Laplacian respectively (see Figures 9(a1) and 9(a2)):

$$\begin{array}{cc}
 \text{Neumann-Dirichlet} & \text{Dirichlet-Neumann} \\
 \text{(a1)} \begin{cases} -\Delta\varphi = \lambda\varphi \text{ in } \Sigma_\alpha^+, \\ \partial_{\mathbf{n}}\varphi = 0 \text{ on } [O, X_0^\alpha], \\ \varphi = 0 \text{ elsewhere.} \end{cases} & \text{(a2)} \begin{cases} -\Delta\varphi = \lambda\varphi \text{ in } \Sigma_\alpha^+, \\ \partial_{\mathbf{n}}\varphi = 0 \text{ on } [X_0^\alpha, M], \\ \varphi = 0 \text{ elsewhere,} \end{cases}
 \end{array}$$

For each mixed problem, the nodal line of the second eigenvector meets the axis  $\{y = 0\}$  at a point of abscissa denoted by  $y^{ND}(x_\alpha)$  and  $y^{DN}(x_\alpha)$  respectively. The choice of the interior singular point  $X_0^\alpha$  gives a 3-partition after symmetrization if and only if

- $y^{ND}(x_\alpha) \geq x_\alpha$  in the Neumann-Dirichlet case,
- $y^{DN}(x_\alpha) \leq x_\alpha$  in the Dirichlet-Neumann case.

Figure 10 gives examples of nodal partitions for several values of  $x_\alpha$ . The Dirichlet condition on the boundary are represented in blue line and the Neumann condition in red dotted line. The nodal line is plotted in black. For the Neumann-Dirichlet configuration (see Figure 10(a)), we obtain a 2-partition after symmetrization if  $x_\alpha$  is too large. If  $x_\alpha$  is such that  $x_\alpha < y^{ND}(x_\alpha)$ , we obtain a 3-partition whose energy can be reduced by removing the Dirichlet line ( $Y^{ND}(x_\alpha), X_0^\alpha$ ) (where  $Y^{ND}(x_\alpha)$  is the point of coordinates  $(y^{ND}(x_\alpha), 0)$ ) in this sub-domain of the partition. We can make a similar analysis in the Dirichlet-Neumann case (see Figure 10(b)).

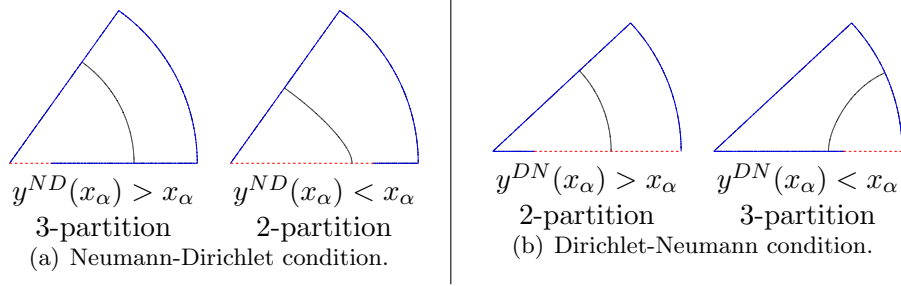


Figure 10: Examples of nodal partition for the mixed problems.

Since the function  $x \mapsto \lambda_2^{ND}(x)$  is decreasing with  $x$  and  $x \mapsto \lambda_2^{DN}(x)$  is increasing with  $x$ , the optimal singular points are:

$$x_\alpha^{ND} = \max\{x_\alpha : y^{ND}(x_\alpha) \geq x_\alpha\}, \quad x_\alpha^{DN} = \min\{x_\alpha : y^{DN}(x_\alpha) \leq x_\alpha\}. \quad (5.1)$$

For numerical simulations, we use the discretization

$$\alpha \in \left\{ \frac{k}{100}\pi, 16 \leq k \leq 77 \right\} \quad \text{and} \quad x_\alpha \in \left\{ \frac{j}{100}, 0 \leq j \leq 100 \right\}.$$

We denote by  $\tilde{x}_\alpha^{ND}$  and  $\tilde{x}_\alpha^{DN}$  the singular points defined by (5.1) for a discretization  $x_\alpha \in \left\{ \frac{j}{100}, 0 \leq j \leq 100 \right\}$ . Figure 11 represents these singular points according to  $\alpha$ .

The 3-partitions obtained after symmetrization give upper-bounds for  $\mathfrak{L}_3(\alpha)$  as illustrated in Figure 12. We observe that the energy for the Neumann-Dirichlet Laplacian is smaller than the one obtained with the Dirichlet-Neumann Laplacian and smaller than  $L_3(\alpha)$ . Thus using Theorem 1.14, we deduce

**Proposition 5.1** *For any  $\alpha \in (\alpha_3^1, \alpha_3^2)$ ,*

$$\lambda_3(\alpha) < \mathfrak{L}_3(\Sigma_\alpha) \leq L_3^{sym}(\alpha) < L_3(\alpha),$$

with  $L_3^{sym}(\alpha) := \min(\lambda_2^{DN}(x_\alpha^{DN}), \lambda_2^{ND}(x_\alpha^{ND})) = \lambda_2^{ND}(x_\alpha^{ND})$ .

Figure 13 gives examples of minimal symmetric 3-partitions of type (a) for several angles. We denote by  $\mathcal{D}_\alpha^{sym}$  the best candidate obtained like this.

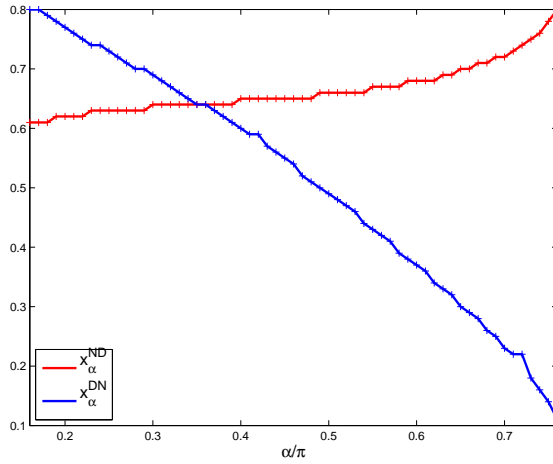


Figure 11:  $\tilde{x}_\alpha^{ND}$  and  $\tilde{x}_\alpha^{DN}$  vs.  $\alpha \in \{k\pi/100, 16 \leq k \leq 77\}$ .

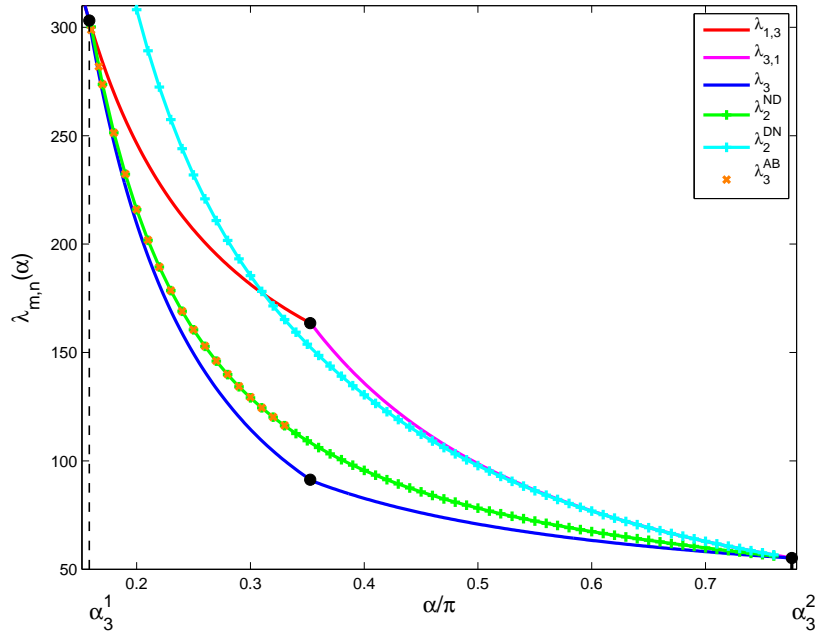


Figure 12: Upper-bound of  $\mathfrak{L}_3(\Sigma_\alpha)$  using symmetric partitions.

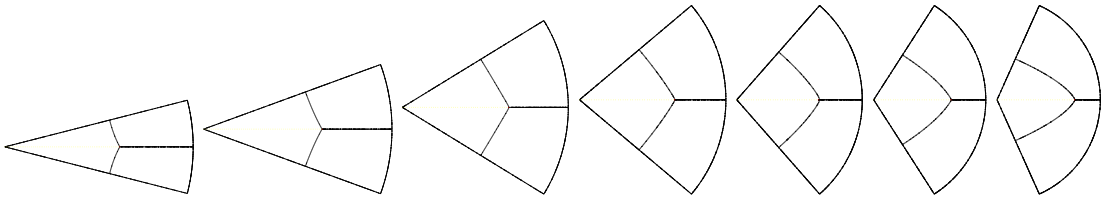


Figure 13: Best candidates for symmetric 3-partition.

## 5.2 Partition with two interior singular points

We have now to deal with the other configurations (b) and (c). Then, as illustrated in Figure 9, the two interior singular points  $X_0$  and  $X_1$  are either on the axis  $\{y = 0\}$ , or



symmetric to each other. Their coordinates are therefore:

1.  $X_0 = (x_0, 0)$  and  $X_1 = (x_1, 0)$  in case (b1) or (c1),
2.  $X_0 = (x_0, y_0)$  and  $X_1 = (x_0, -y_0)$  in case (b2) or (c2).

Let us first rule out configurations (b2) and (c2):

**Lemma 5.2** *Let  $\alpha \in (\alpha_3^1, \alpha_3^2)$  and  $\mathcal{D}_\alpha$  be a minimal 3-partition. We assume that this partition is symmetric according to the  $y$ -axis. Then the interior singular points are necessarily on the axis  $\{y = 0\}$ .*

**Proof:** This is clear for configuration of type (a) and we have used this property previously. Let us now assume that the partition  $\mathcal{D}_\alpha$  is of type (b2) or (c2). Then, since  $\mathcal{D}_\alpha^+ = \mathcal{D}_\alpha \cap \{y > 0\}$  is a 3-partition with Neumann condition on the symmetry axis  $\{y = 0\}$ , we infer, by the min-max principle,

$$\Lambda_3(\mathcal{D}_\alpha) \geq \lambda_3^N(\alpha),$$

where  $\lambda_3^N(\alpha)$  is the third eigenvalue on  $\Sigma_\alpha^+$  with Neumann condition on  $\{y = 0\}$  and Dirichlet condition elsewhere. But  $\lambda_3^N(\alpha) = \lambda_{1,3}(\alpha)$  if  $\alpha_3^1 < \alpha \leq \beta_3$  and  $\lambda_3^N(\alpha) = \lambda_{3,1}(\alpha)$  if  $\beta_3 \leq \alpha < \alpha_3^2$ , that is to say

$$\lambda_3^N(\alpha) = L_3(\alpha), \quad \forall \alpha \in (\alpha_3^1, \alpha_3^2).$$

Using Proposition 5.1 and Figure 12, we observe that for any  $\alpha \in (\alpha_3^1, \alpha_3^2)$ , we find a symmetric 3-partition  $\mathcal{D}_\alpha^{sym}$  of type (a1) such that

$$\Lambda_3(\mathcal{D}_\alpha^{sym}) < L_3(\alpha) \leq \Lambda_3(\mathcal{D}_\alpha).$$

Thus  $\mathcal{D}_\alpha$  cannot be a minimal 3-partition. ■

We have then reduced the study to configurations (b1) and (c1). The associated mixed problems read

Neumann-Dirichlet-Neumann	Dirichlet-Neumann-Dirichlet
$(b1) \begin{cases} -\Delta\varphi = \lambda\varphi \text{ in } \Sigma_\alpha^+, \\ \partial_{\mathbf{n}}\varphi = 0 \text{ on } [O, X_0^\alpha] \cup [X_1^\alpha, M], \\ \varphi = 0 \text{ elsewhere,} \end{cases}$	$(c1) \begin{cases} -\Delta\varphi = \lambda\varphi \text{ in } \Sigma_\alpha^+, \\ \partial_{\mathbf{n}}\varphi = 0 \text{ on } [X_0^\alpha, X_1^\alpha], \\ \varphi = 0 \text{ elsewhere.} \end{cases}$

Using the results of Subsection 5.1 for the configuration (a), we can restrict the possible critical points for configuration (c1):

**Proposition 5.3** *Let  $\mathcal{D} = (D_1, D_2, D_3)$  be a symmetric 3-partition of type (c1) with the interior singular points  $X_0^\alpha$  and  $X_1^\alpha$  of coordinates  $(x_0, 0)$  and  $(x_1, 0)$ . We assume either  $x_0 < x_1 \leq x_\alpha^{ND}$ , or  $x_\alpha^{DN} \leq x_0 < x_1$ . Then this partition cannot be minimal.*

**Proof:** We assume that  $x_0 < x_1 < x_\alpha^{ND}$  and that  $D_1 \subset \{y > 0\}$  and  $D_3^+ = D_3 \cap \{y > 0\} \neq \emptyset$ . Then the partition  $\mathcal{D}^+ = (D_1, D_3^+)$  satisfies the Dirichlet-Neumann-Dirichlet problem (c1) and we have then, by the min-max principle,

$$\Lambda_3(\mathcal{D}) \geq \lambda_2^{DND}(x_0, x_1),$$

with  $\lambda_2^{DND}(x_0, x_1)$  the second eigenvalue of the Dirichlet-Neumann-Dirichlet Laplacian (c1) on  $\Sigma_\alpha^+$ . By monotonicity due to the Dirichlet condition and since  $x_0 < x_1 \leq x_\alpha^{ND}$ , we have

$$\lambda_2^{DND}(x_0, x_1) > \lambda_2^{ND}(x_1) \geq \lambda_2^{ND}(x_\alpha^{ND}) = L_3^{sym}(\alpha) \geq \mathfrak{L}_3(\alpha).$$

Thus the partition  $\mathcal{D}$  can not be minimal.

The proof is similar if we assume  $x_\alpha^{DN} \leq x_0 < x_1$ . ■

Figure 11 gives an approximation at  $1/100$  for  $x_\alpha^{ND}$  and  $x_\alpha^{DN}$  and thus the location for possible interior singular points for configuration (c1).

When we search for candidates of type (b1) or (c1) numerically, we use the discretization

$$\alpha \in \left\{ \frac{k}{100}\pi, 16 \leq k \leq 77 \right\} \quad \text{and} \quad X_k^\alpha = (x_k^\alpha, 0), \quad x_k^\alpha \in \left\{ \frac{j}{100}, 0 \leq j \leq 100 \right\}, \quad k = 0, 1.$$

As in [5] for the square and the disk, the second eigenfunction associated with these mixed problems never produces a configuration of type (b) or (c). Then the mixed Neumann-Dirichlet problem provides the best symmetric candidates for any  $\alpha \in (\alpha_3^1, \alpha_3^2)$ .

### 5.3 Angular sector of opening $\alpha = \pi/3$

Let us analyze more specifically the case  $\alpha = \pi/3$ . Using the approach developed in Subsection 5.1, the best candidate obtained is represented in Figure 14 with  $\tilde{x}_{\pi/3}^{ND} = 0.64$  (we recall that for the numerics,  $x_\alpha \in \{k/100, 0 \leq k \leq 100\}$ ). It seems that the nodal lines are straight lines. This is compatible with the equal angle properties: At the interior singular point, the nodal lines have to meet with angle  $2\pi/3$  whereas the nodal lines meet the boundary at right angles.

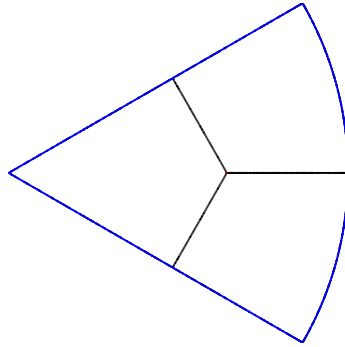


Figure 14: Symmetric candidate for  $\Sigma_{\pi/3}$ .

Let us try to understand some properties of such a partition. We reproduce this 3-partition of  $\Sigma_{\pi/3}$  by rotation of  $\pm\pi/3$  and  $\pm 2\pi/3$  to tile the disk. Figure 15 represents this tiling of the disk. Let us compare the areas of the sub-domains  $(\Omega_1, \Omega_2, \Omega_3)$  of the partition

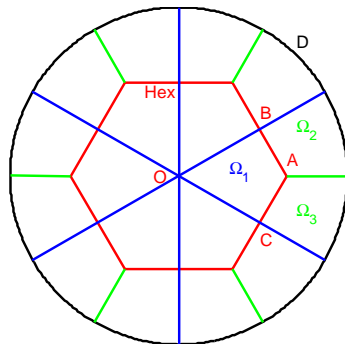


Figure 15: Tiling of the disk with the 3-partition of Figure 14.

of  $\Sigma_{\pi/3}$ , assuming that the nodal lines are straight lines. We denote by  $A$  the interior singular point of coordinates  $(L, 0)$ . Let  $B$  be the boundary singular point of coordinates  $L/4(3, \sqrt{3})$  and  $C$  its symmetric point according to the axis  $\{y = 0\}$ . The area of the total disk  $Disk$  equals  $\mathcal{A}(Disk) = \pi$ . The area of the regular hexagon plotted in red in Figure 15 is

$$\mathcal{A}(\text{Hex}) = \frac{3\sqrt{3}}{2}L^2.$$

We deduce

$$\mathcal{A}(\Omega_1) = \frac{\sqrt{3}L^2}{4}.$$

Let us now compute the area of  $\Omega_2$ . We have

$$\mathcal{A}(\Omega_2) = \frac{1}{12}(\mathcal{A}(Disk) - \mathcal{A}(\text{Hex})) = \frac{2\pi - 3\sqrt{3}L^2}{24}.$$

With  $L = 0.64$ , we obtain

$$\mathcal{A}(\Omega_1) \simeq 0.177 \quad \text{and} \quad \mathcal{A}(\Omega_2) \simeq 0.173.$$

Since the accuracy on  $L$  is  $10^{-2}$ , this gap is not significant. Let us determine now for which value of  $L$  we have the equality:

$$\mathcal{A}(\Omega_1) = \mathcal{A}(\Omega_2) \iff \frac{\sqrt{3}L^2}{4} = \frac{2\pi - 3\sqrt{3}L^2}{24} \iff L = \sqrt{\frac{2\pi}{9\sqrt{3}}} \simeq 0.634\ 875.$$

In this case, we have  $\mathcal{A}(\text{Hex}) = \pi/3$ .

This result is coherent with the discretization step for  $x_\alpha$  which equals  $1/100$ . Therefore it seems that the areas of every domains of the partition are equal.

## 6 Laplacian on the double covering

The method proposed in Section 5 can only catch symmetric candidates. However, we have seen in Figure 7 that for the angle  $\alpha = \alpha_3^1$ , there exists non symmetric minimal 3-partitions. So we would like to find a method to catch non symmetric candidates. The method we use now was introduced in [4] to explain why we find two symmetric configurations with the same energy in the square. Let us explain this method. Let us go back to a general bounded open and simply connected set  $\Omega$  with piecewise  $C^{1,+}$  boundary. In the non nodal case, there are three topological types possible for a minimal 3-partition of such a domain. They are given by configuration (a), (b), and (c) in Section 5, removing the symmetry assumption. As suggested by the numerical study of the symmetric case, we only look for minimal partitions of type (a). Then, there is an interior singular point where three half-curves meet. Following [4], we consider a double Riemannian covering of the domain  $\Omega$  punctured by this point. We then look for a minimal partition of  $\Omega$  as the projection of a nodal partition of the double covering.

### 6.1 Double covering of the domain

We will give a rather informal description of the double covering. Let us consider a point  $X_0 \in \Omega$ . We denote  $\Omega \setminus \{X_0\}$  by  $\Omega_{X_0}$ . We now choose a simple regular curve  $\gamma$  contained in  $\Omega$  that links  $X_0$  to a point in  $\partial\Omega$ . We consider two copies of  $\Omega \setminus \gamma$  that we glue in such a way that a side of  $\gamma$  on one sheet is connected to the opposite side on the other sheet

(cf. Figure 16). The resulting object is a two dimensional manifold with boundary, that we denote by  $\tilde{\Omega}_{X_0}$ , with a natural projection map  $\Pi : \tilde{\Omega}_{X_0} \rightarrow \Omega_{X_0}$ . It is a double covering of  $\Omega_{X_0}$ , that we equip with the Riemannian metric lifted from  $\Omega_{X_0}$  through  $\Pi$ . A rigorous and general construction is explained in [12]. In particular, it can be shown that the result does not depend on the choice of  $\gamma$ .

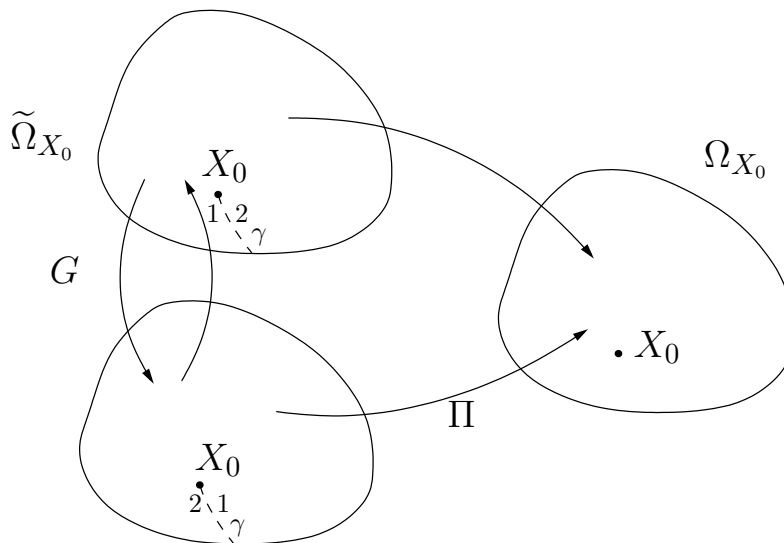


Figure 16: Double covering of  $\Omega_{X_0}$ .

## 6.2 Symmetric and antisymmetric eigenvalues

Let us now define a mapping  $G$  from  $\tilde{\Omega}_{X_0}$  onto itself, called the *deck map*. For any  $X_1 \in \tilde{\Omega}_{X_0}$ ,  $G(X_1)$  is the only element  $X_2 \in \tilde{\Omega}_{X_0}$  such that  $X_2 \neq X_1$  and  $\Pi(X_2) = \Pi(X_1)$ . Intuitively, the mapping  $G$  moves points from one sheet of the double covering to the other one. We have of course  $G^2 = \text{Id}$ . A function  $f : \tilde{\Omega}_{X_0} \rightarrow \mathbb{C}$  is said to be *symmetric* if  $f \circ G = f$  and *antisymmetric* if  $f \circ G = -f$ . If we call  $\mathcal{S}$  (resp.  $\mathcal{A}$ ) the space of functions in  $L^2(\tilde{\Omega}_{X_0})$  that are symmetric (resp. antisymmetric), we have the orthogonal decomposition:

$$L^2(\tilde{\Omega}_{X_0}) = \mathcal{S} \oplus \mathcal{A}.$$

We call *lifted Laplacian* the Laplace-Beltrami operator on  $\tilde{\Omega}_{X_0}$  with Dirichlet boundary condition. The lifted Laplacian preserves symmetric and antisymmetric functions. We can therefore choose a basis of eigenfunctions for each subspace  $\mathcal{S}$  and  $\mathcal{A}$ . Their reunion is a basis of eigenfunctions for  $L^2(\tilde{\Omega}_{X_0})$ . The eigenvalues associated with a symmetric (resp. antisymmetric) eigenfunction will be called *symmetric* (resp. *antisymmetric*). The symmetric eigenvalues are actually the eigenvalues of the Dirichlet Laplacian on  $\Omega$ , since any symmetric eigenfunction is lifted from an eigenfunction on  $\Omega_{X_0}$ . We call the antisymmetric eigenvalues *Aharonov-Bohm eigenvalues*, denoted by  $\lambda_k^{AB}$ , since they can be considered as the eigenvalues of a so-called *Aharonov-Bohm operator* with pole at  $X = X_0$  and flux  $\Phi = 1/2$  (cf. [1, 12, 2, 18]).

Let us now consider a nodal partition  $\mathcal{D} = \{D_i : 1 \leq i \leq \ell\}$  associated with an antisymmetric eigenfunction  $u$ . The image of a domain of  $\mathcal{D}$  by the deck map  $G$  is another domain where  $u$  has the opposite sign. We can therefore group together the domains of  $\mathcal{D}$  in pairs  $\{D_i, D_j\}$  such that  $D_i \cap D_j = \emptyset$  and  $\Pi(D_i) = \Pi(D_j)$ . The set  $\Pi(\mathcal{D}) = \{\Pi(D_i) : 1 \leq i \leq \ell\}$

is then a strong  $k$ -partition of  $\Omega$ , with  $2k = \ell$  (we deduce in particular that  $\ell$  is even). Furthermore, contrary to  $\mathcal{D}$ , the partition  $\Pi(\mathcal{D})$  is not necessarily bipartite. We will use this to build non nodal candidates to be a minimal  $k$ -partition.

Consequently, if we find for some  $\alpha$  a singular point  $X$  such that there exists an antisymmetric eigenfunction with 6 nodal domains and associated with  $\lambda_6((\widetilde{\Sigma}_\alpha)_X)$  such that

$$\lambda_6((\widetilde{\Sigma}_\alpha)_X) < \Lambda_3(\mathcal{D}_\alpha^{sym}),$$

then the symmetric 3-partition  $\mathcal{D}_\alpha^{sym}$  is not minimal. Indeed, the projection of this sixth eigenfunction on the first sheet is a 3-partition whose energy is less than  $\Lambda_3(\mathcal{D}_\alpha^{sym})$ .

We have another way of checking that a 3-partition is not minimal. According to [13, Remark 5.2], a minimal 3-partition must be Courant-sharp for the Aharonov-Bohm operator, that is to say, its energy must be  $\lambda_3^{AB}$ .

Let us now combine the double covering approach and the results of Section 5 to obtain more information. The first result consists in invalidating possibly some candidates of type (a1) obtained in Subsection 5.1. Let us use the best candidates obtained in Subsection 5.1. For any  $\alpha \in \{k\pi/100, 16 \leq k \leq 76\}$ , we compute the first eigenvalues of the Dirichlet Laplacian on the double covering  $(\widetilde{\Sigma}_\alpha)_X$  with  $X = (\tilde{x}_\alpha^{ND}, 0)$  and we split the spectrum between the symmetric eigenvalues  $\lambda_k((\widetilde{\Sigma}_\alpha)_X)$  and the antisymmetric ones  $\lambda_k^{AB}((\widetilde{\Sigma}_\alpha)_X)$ . Figure 17 gives the first seven eigenvalues on  $(\widetilde{\Sigma}_\alpha)_X$  and the nodal partition of the eigen-

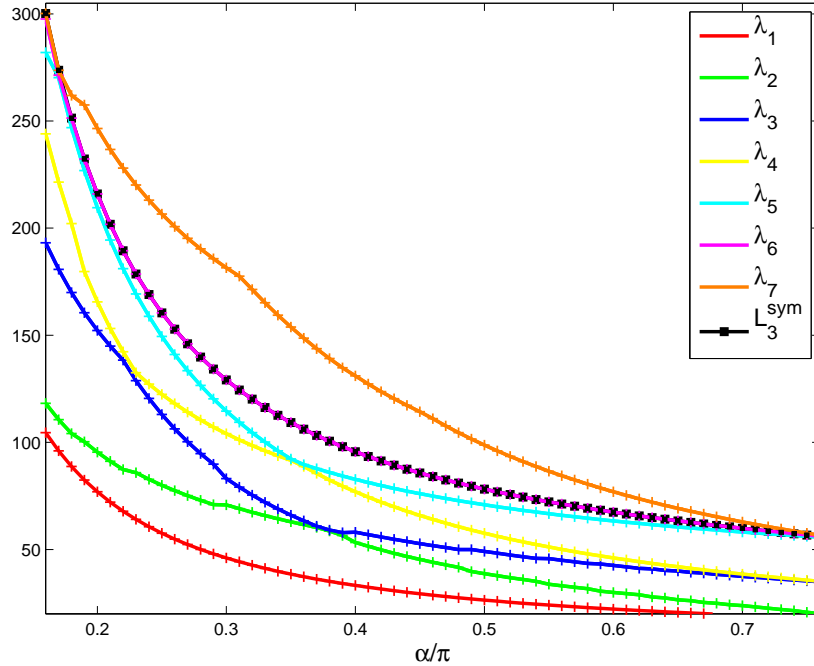


Figure 17:  $\lambda_j((\widetilde{\Sigma}_\alpha)_X)$ , with  $X = (\tilde{x}_\alpha^{ND}, 0)$ ,  $\alpha \in \{k\pi/100, 16 \leq k \leq 76, 1 \leq j \leq 7\}$ .

functions are represented on Figure 18 for several  $\alpha$ . We notice that

$$\Lambda_3(\mathcal{D}_\alpha^{sym}) = \lambda_7((\widetilde{\Sigma}_\alpha)_X) = \lambda_4^{AB}((\Sigma_\alpha)_X) > \lambda_5((\widetilde{\Sigma}_\alpha)_X) = \lambda_3^{AB}((\Sigma_\alpha)_X), \text{ for } \alpha = 16\pi/100,$$

$$\Lambda_3(\mathcal{D}_\alpha^{sym}) = \lambda_7((\widetilde{\Sigma}_\alpha)_X) = \lambda_4^{AB}((\Sigma_\alpha)_X) > \lambda_6((\widetilde{\Sigma}_\alpha)_X) = \lambda_3^{AB}((\Sigma_\alpha)_X), \text{ for } \alpha = 17\pi/100,$$

$$\Lambda_3(\mathcal{D}_\alpha^{sym}) = \lambda_6((\widetilde{\Sigma}_\alpha)_X) = \lambda_3^{AB}((\Sigma_\alpha)_X), \text{ for } \alpha \in \{k\pi/100, k = 18, \dots, 76\}.$$

Consequently, the minimal symmetric 3-partition  $\mathcal{D}_\alpha^{sym}$  is not minimal for  $\alpha = 16\pi/100$  and  $\alpha = 17\pi/100$ .

To make simulations, we use the techniques we have previously explained in [3]: this consists in meshing the double covering for the domain and using the Finite Element Library MÉLINA (see [16]).

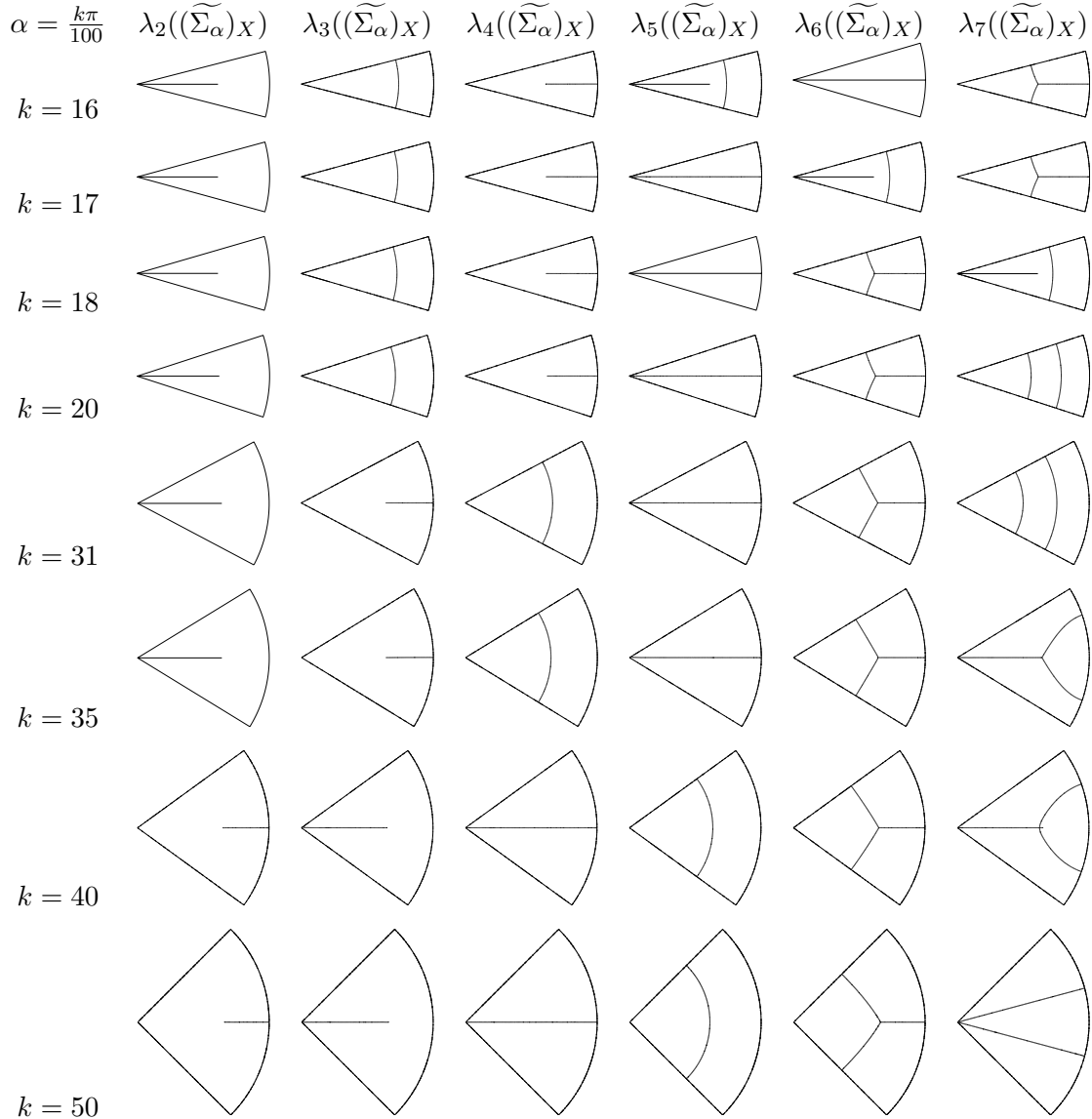


Figure 18: Nodal partition associated with  $\lambda_j((\widetilde{\Sigma}_\alpha)_X)$ ,  $X = (\tilde{x}_\alpha^{ND}, 0)$ ,  $\alpha = \frac{k\pi}{100}$ ,  $2 \leq j \leq 7$ .

### 6.3 Numerical simulations for non symmetric candidates

Let us consider an angle  $\alpha = \alpha_3^1 + \varepsilon$  with  $\varepsilon$  very small and positive. We have seen that the 3-partition  $\mathcal{D}_\alpha^{sym}$  is not minimal when  $\varepsilon$  is small enough.

We would like to use the double covering approach to catch some non symmetric candidates. For any point  $X \in \Omega$ , we compute the first six eigenvalues of the Dirichlet Laplacian on the double covering  $(\widetilde{\Sigma}_\alpha)_X$ . The symmetric eigenvectors are those of the Dirichlet Laplacian on  $\Sigma_\alpha$  and we are interested in the antisymmetric ones. We move the

puncturing point on  $\Sigma_\alpha$  and hope to find a 3-partition given by the 6-th eigenfunction of the Dirichlet Laplacian on  $(\widehat{\Sigma_\alpha})_X$ .

Proposition 4.1 gives us an idea to localize the puncturing point  $X$ . Starting with  $\Sigma_\alpha$  for  $\alpha = \alpha_3^1$ , we can pick an eigenfunction whose nodal set has a boundary singular point with polar coordinates  $(\rho_c, \alpha_3^1/2)$ . Its nodal partition has three domains and a boundary singular point at  $(\rho_c, \alpha_3^1/2)$  where two lines meet. We recall that at a singular point, nodal lines satisfy the equal angle property. We can use this property to localize a possible singular point for  $\Sigma_\alpha$  with  $\alpha = \alpha_3^1 + \varepsilon$ . If the minimal 3-partition for  $\Sigma_\alpha$  has a singular point on the boundary  $\{y = x \tan \frac{\alpha}{2}\}$  with only one nodal line reaching this point, then this nodal line is normal to the boundary at the singular point. If  $\varepsilon$  is very small, the distance between this singular point and the origin should be close to  $\rho_c$ .

When the angle is increasing, this approximation is not efficient. For  $\alpha = \pi/3$ , the boundary singular point seems to have polar coordinates  $(\rho_3, \pi/6)$  with  $\rho_3 = L\sqrt{3}/2 \simeq 0.5498$ .

For numerical computations, we choose  $X$  on some perpendicular axes to the boundary (see Figure 19):

$$X \in \{X_k = (1 - \frac{k}{100})C_\rho + \frac{k}{100}A_\rho, 0 \leq k \leq 100\},$$

where  $C_\rho$  and  $A_\rho$  are the points of coordinates

$$C_\rho = \rho(\cos \frac{\alpha}{2}, \sin \frac{\alpha}{2}) \text{ and } A_\rho = \rho(1/\cos \frac{\alpha}{2}, 0), \quad \text{with } \rho \in \{0.54 + k/50, k = 0, \dots, 6\}.$$

Then we catch a 3-partition among the 6-th eigenfunction of the Dirichlet Laplacian on  $(\widehat{\Sigma_\alpha})_X$ . With this method, we obtain, for several values of  $\alpha$ , new partitions  $\mathcal{D}_\alpha^{AB}$  better than the minimal symmetric 3-partition  $\mathcal{D}_\alpha^{sym}$  obtained by the mixed Neumann-Dirichlet approach (see Figure 20).

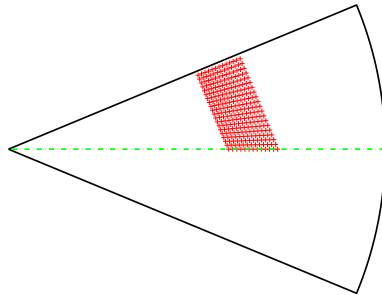


Figure 19: Localization of the puncturing point for numerical simulations,  $\alpha = 0.5$ .

For different sectors, we proceed in the same way and obtain new candidates whose energy is represented in orange color in Figure 12 (see also Figure 20). We obtain a better candidate than the symmetric one for angles close to  $\alpha_3^1$  and especially for  $\alpha = 16\pi/100$  and  $\alpha = \pi/6$ . For larger angles, the double covering approach gives candidates whose energy is so close to those of the symmetric candidates that we cannot be affirmative. This is probably due to the fact that the best candidate obtained by the double covering approach has an interior singular point close to (or on) the symmetry axis for larger  $\alpha$  and then, by continuity, the eigenvalues are close to those of the mixed Neumann-Dirichlet Laplacian.

Notice that for  $\alpha = \alpha_3^2$ , all candidates in Figure 8 are symmetric. This encourages us to make the conjecture:

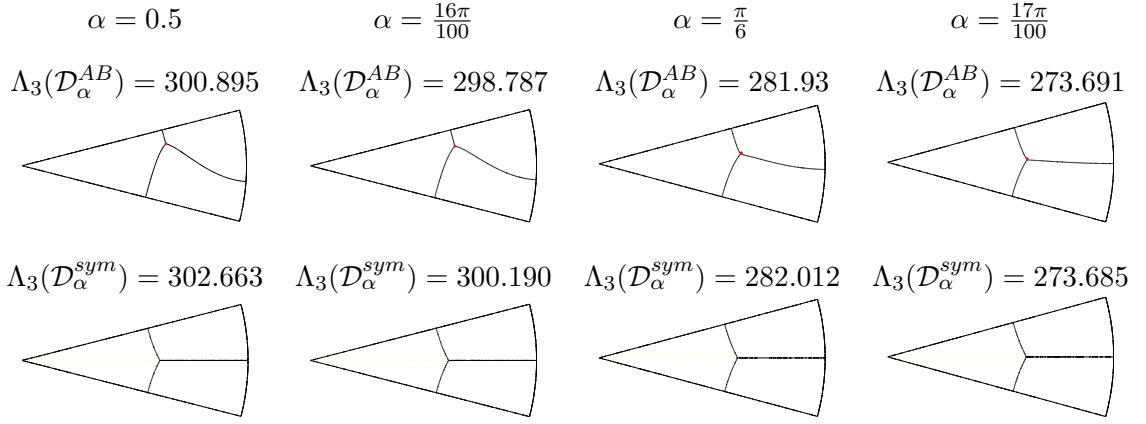


Figure 20: Candidates for the minimal 3-partition of  $\Sigma_\alpha$ .

**Conjecture 6.1** *There exists  $\alpha_3^3$  such that*

- *for  $\alpha \in (\alpha_3^1, \alpha_3^3)$ , the minimal 3-partitions are non symmetric,*
- *for  $\alpha \in (\alpha_3^3, \alpha_3^2)$ , any minimal 3-partition is symmetric.*

## 7 Negative results for minimal $k$ -partitions, $k = 4, 5, 6$

### 7.1 4-partition

Figure 21 illustrates the lower and upper bounds for  $\mathfrak{L}_4(\Sigma_\alpha)$ :

$$\lambda_4(\alpha) \leq \mathfrak{L}_4(\Sigma_\alpha) \leq \min(\lambda_{1,4}(\alpha), \lambda_{2,2}(\alpha), \lambda_{4,1}(\alpha)).$$

We observe that  $\lambda_{2,2}(\alpha) > \lambda_4(\alpha)$ . Consequently, partitions having the topology illustrated in Figure 22 cannot be minimal for any  $\alpha$ .

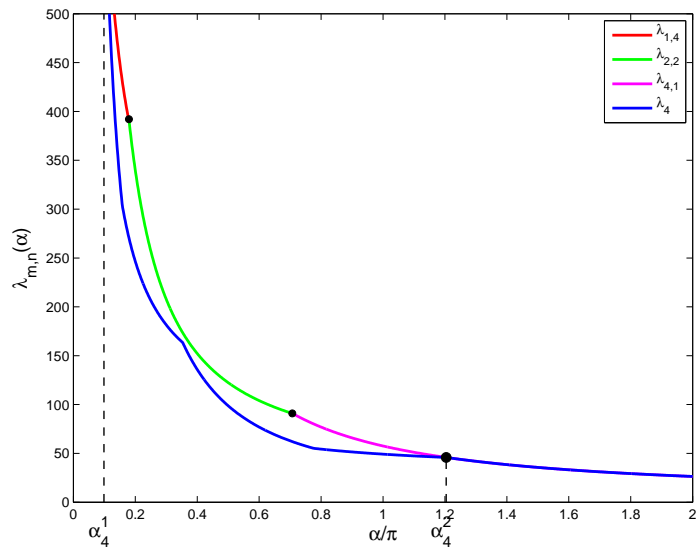


Figure 21: Bounds for  $\mathfrak{L}_4(\Sigma_\alpha)$ .



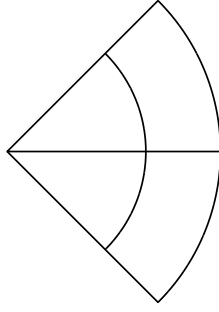


Figure 22: Non minimal 4-partition.

## 7.2 5-partition

Since  $k = 5$  is a prime number, we only have the bounds given by Proposition 3.2 and Remark 3.3:

$$\begin{aligned} \mathfrak{L}_5(\alpha) &= \lambda_5(\alpha) && \text{for } \alpha \in (0, \alpha_5^1] \cup [\alpha_5^2, 2\pi], \\ \lambda_5(\alpha) < \mathfrak{L}_5(\alpha) < L_5(\Sigma_\alpha) &\leq \min(\lambda_{1,5}(\alpha), \lambda_{5,1}(\alpha)) && \text{for } \alpha \in (\alpha_5^1, \alpha_5^2). \end{aligned}$$

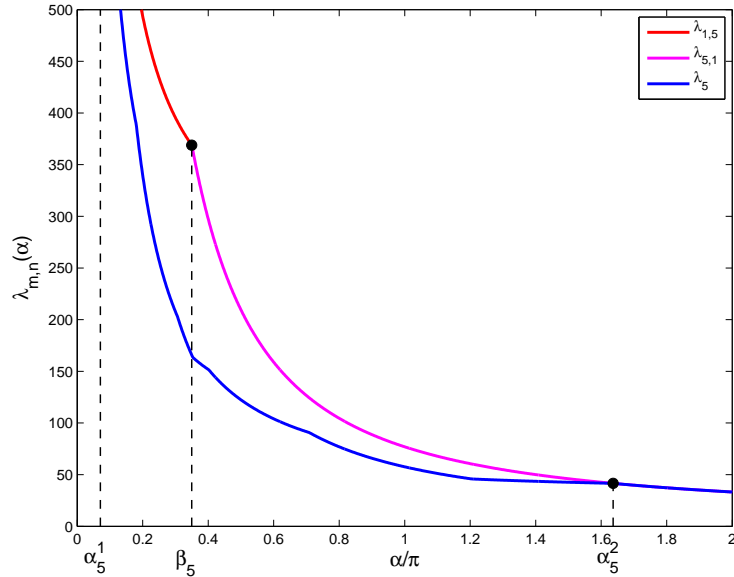


Figure 23: Bounds for  $\mathfrak{L}_5(\Sigma_\alpha)$ .

## 7.3 6-partition

Using Figure 24, we notice that

$$\min(\lambda_{2,3}(\alpha), \lambda_{3,2}(\alpha), \lambda_{6,1}(\alpha)) > \lambda_6(\alpha), \quad \forall \alpha \in (0, 2\pi].$$

Thus candidates of the types illustrated in Figure 25 are never minimal.

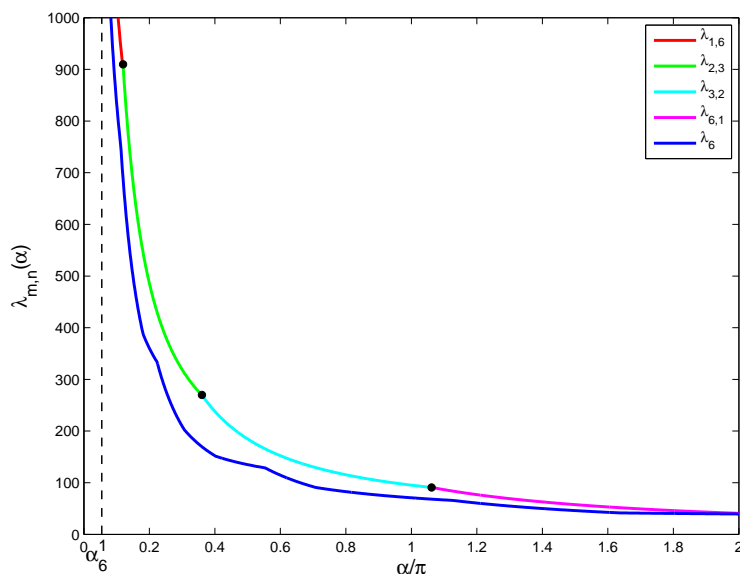


Figure 24: Bounds for  $\mathfrak{L}_6(\Sigma_\alpha)$ .

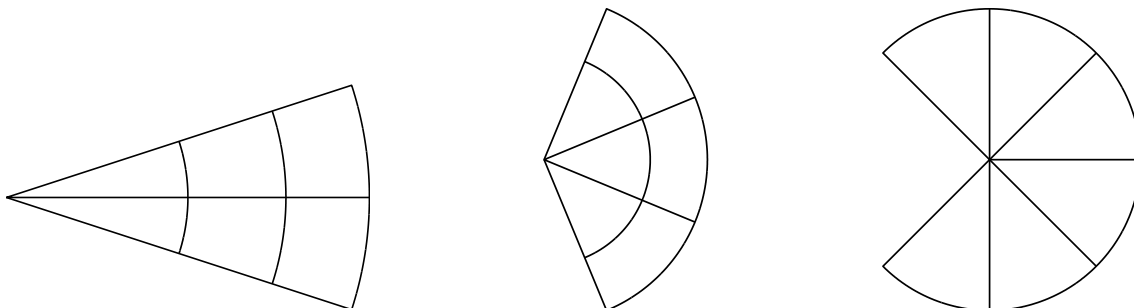


Figure 25: Non minimal 6-partitions.

**Acknowledgements.** The authors thank Bernard Helffer for many suggestions and discussions concerning this work. This work was partially supported by the ANR (Agence Nationale de la Recherche), projects GAOS n° ANR-09-BLAN-0037-03 and OPTIFORM n° ANR-12-BS01-0007-02. The first author is grateful to the Mittag-Leffler Institute where this paper was achieved.

## References

- [1] Y. AHARONOV, D. BOHM. Significance of electromagnetic potentials in the quantum theory. *Phys. Rev.* **115** (Aug 1959) 485–491.
- [2] B. ALZIARY, J. FLECKINGER-PELLÉ, P. TAKÁČ. Eigenfunctions and Hardy inequalities for a magnetic Schrödinger operator in  $\mathbb{R}^2$ . *Math. Methods Appl. Sci.* **26**(13) (2003) 1093–1136.
- [3] V. BONNAILLIE-NOËL, B. HELFFER. Numerical analysis of nodal sets for eigenvalues of Aharonov-Bohm Hamiltonians on the square with application to minimal partitions. *Exp. Math.* **20**(3) (2011) 304–322.

- [4] V. BONNAILLIE-NOËL, B. HELFFER, T. HOFFMANN-OSTENHOF. Aharonov-Bohm Hamiltonians, isospectrality and minimal partitions. *J. Phys. A* **42**(18) (2009) 185203, 20.
- [5] V. BONNAILLIE-NOËL, B. HELFFER, G. VIAL. Numerical simulations for nodal domains and spectral minimal partitions. *ESAIM Control Optim. Calc. Var.* **16**(1) (2010) 221–246.
- [6] D. BUCUR, G. BUTTAZZO, A. HENROT. Existence results for some optimal partition problems. *Adv. Math. Sci. Appl.* **8**(2) (1998) 571–579.
- [7] M. CONTI, S. TERRACINI, G. VERZINI. An optimal partition problem related to nonlinear eigenvalues. *J. Funct. Anal.* **198**(1) (2003) 160–196.
- [8] M. CONTI, S. TERRACINI, G. VERZINI. On a class of optimal partition problems related to the Fučík spectrum and to the monotonicity formulae. *Calc. Var. Partial Differential Equations* **22**(1) (2005) 45–72.
- [9] M. CONTI, S. TERRACINI, G. VERZINI. A variational problem for the spatial segregation of reaction-diffusion systems. *Indiana Univ. Math. J.* **54**(3) (2005) 779–815.
- [10] R. COURANT, D. HILBERT. *Methods of mathematical physics. Vol. I.* Interscience Publishers, Inc., New York, N.Y. 1953.
- [11] NIST Digital Library of Mathematical Functions. <http://dlmf.nist.gov/>, Release 1.0.5 of 2012-10-01. Online companion to [17].
- [12] B. HELFFER, M. HOFFMANN-OSTENHOF, T. HOFFMANN-OSTENHOF, M. P. OWEN. Nodal sets for groundstates of Schrödinger operators with zero magnetic field in non-simply connected domains. *Comm. Math. Phys.* **202**(3) (1999) 629–649.
- [13] B. HELFFER, T. HOFFMANN-OSTENHOF. On a magnetic characterization of spectral minimal partitions. *Journal of the European Mathematical Society* (À paraître).
- [14] B. HELFFER, T. HOFFMANN-OSTENHOF. On minimal partitions: new properties and applications to the disk. In *Spectrum and dynamics*, volume 52 of *CRM Proc. Lecture Notes*, pages 119–135. Amer. Math. Soc., Providence, RI 2010.
- [15] B. HELFFER, T. HOFFMANN-OSTENHOF, S. TERRACINI. Nodal domains and spectral minimal partitions. *Ann. Inst. H. Poincaré Anal. Non Linéaire* **26**(1) (2009) 101–138.
- [16] D. MARTIN. MÉLINA, bibliothèque de calculs éléments finis.  
<http://perso.univ-rennes1.fr/daniel.martin/melina> (2007).
- [17] F. W. J. OLVER, D. W. LOZIER, R. F. BOISVERT, C. W. CLARK, editors. *NIST Handbook of Mathematical Functions*. Cambridge University Press, New York, NY 2010. Print companion to [11].
- [18] K. PANKRASHKIN, S. RICHARD. Spectral and scattering theory for the Aharonov-Bohm operators. *Rev. Math. Phys.* **23**(1) (2011) 53–81.